Mechanisms of 4-phenylazophenol elimination in micro- and nano-ZVI assisted-Fenton systems

Jorge A. Donadelli[a,*], Bruno Caram[b], Maria Kalaboka[c], Margarita Kapsi[c], Vasilios A. Sakkas[c], Luciano Carlos[d], Fernando S. García Einschlag[b]

[a] *YPF TECNOLOGÍA S. A., Av. Del Petróleo s/n (Entre 129 y 143), Berisso, Argentina*
[b] *Instituto De Investigaciones Fisicoquímicas Teóricas y Aplicadas (INIFTA), CCT-La Plata-CONICET, Universidad Nacional De La Plata, Diag 113 y 64, La Plata, Argentina*
[c] *Department of Chemistry, University of Ioannina, Panepistimioupolis, Ioannina 45110, Greece*
[d] *Instituto De Investigación y Desarrollo En Ingeniería De Procesos, Biotecnología y Energías Alternativas, PROBIEN (CONICET-UNCo), Buenos Aires 1400, Neuquén, Argentina*

ARTICLE INFO

ABSTRACT

The 4-phenylazophenol (4-PAP), was treated with two different sources of metallic iron (ZVI): commercial micrometric powder (pZVI) and nanoparticles synthetized by the borohydride reduction method (nZVI). 4-PAP degradation was studied both in the absence and in the presence of H_2O_2 at different pHs. The degradation products of 4-PAP in each treatment were followed by LC-MS and CG-MS. Results showed that, in the absence of H_2O_2, the azo bond reduction of 4-PAP with the formation of amines was the main mechanism involved for both ZVI sources and nZVI exhibited a faster substrate removal than pZVI. In the presence of H_2O_2, an additional mechanism involving the oxidation mediated by hydroxyl radicals takes place. For pZVI, the addition of H_2O_2 produced a complete inhibition of the reduction pathway, being the oxidation the main degradation mechanism. In the case of nZVI, the system behavior showed an important dependence on the working pH. At pH 3.00, oxidative transformation pathways prevailed, whereas at pH 5.00 an almost negligible degradation -mainly driven by 4-PAP reduction- was observed. The assessment of the involved reaction mechanisms under different conditions allows the selection of the most suitable source for a specific treatment.

1. Introduction

Fenton related techniques are one of the most studied wastewater treatments due to their ability to oxidize a wide variety of pollutants using green reactants with few environmental impacts [1]. Several works have focused on its use for the degradation of azo dyes [2–4], the most common family of dyes used in textile industry [5]. These dyes are resistant to traditional biological treatments and can generate carcinogenic aromatic amines upon reduction [6]. In particular, it has been shown that the dye 4-phenylazophenol (4-PAP), also known as Solvent Yellow 7, may be easily absorbed by human skin and metabolized to the mutagenic aniline [7]. 4-PAP has one of the simplest structures among azo dyes, consisting on a benzene and a phenol ring conjugated through an azo linkage (Fig. S1). This is an advantage for identification of products obtained under different conditions.

Fenton related techniques are based on the production of hydroxyl radicals (OH˙) from Fe(II) and H_2O_2 [8].

$$Fe(II) + H_2O_2 \rightarrow [Fe(III)OH]^{2+} + HO^{\cdot} \qquad (1)$$
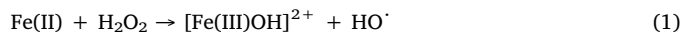
Hydroxyl radicals have a high oxidation potential [9] and are capable of oxidize most of the organic compounds present in industrial effluents. The oxidation of aromatic compounds usually involves the addition of a hydroxyl group (-OH) to the aromatic ring during the first oxidation steps generating hydroxylated derivatives [10]. A subsequent attack of hydroxyl radical produces dihydroxylated compounds. Although a third addition is possible, trihydroxylated compounds are unstable and tend to undergo ring opening reactions with the loss of aromaticity and the generation of aliphatic acids [11]. In the case of azo dyes, OH˙ can also attack azo bonds thus generating hydroxylamines (R-NHOH), hydroxyl hydrazines (R-NH-NHOH), nitroso compounds (R-

---

N = O), diazo compounds (R-N = NH) and keto- imines (R = NH) [12]. Although the oxidation mediated by hydroxyl radicals is the most usual mechanism attributed to Fenton related techniques, it has been reported that in some conditions other oxidant species such as ferryl ion (FeO_2^{2+}) may be formed and participate in the reaction mechanism [13].

ZVI-Assisted Fenton is a variant of Fenton process where the Fe(II) is provided by the oxidation of metallic iron (commonly called Zero Valent Iron, or ZVI) [14,15]. This variant has the advantage of introducing a new removal pathway that involves the reduction of the target pollutant by metallic iron. According to the usually accepted mechanism of azo dyes reduction by ZVI, there is an electron transfer from iron to the nitrogen atoms that leads to the cleavage of the azo bond [16–18].

$$4\text{-PAP} + 2\ Fe^0 + 4H^+ \rightarrow \text{Aniline} + \text{4-OH-aniline} + 2\ Fe(II) \qquad (2)$$
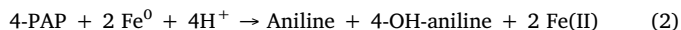
In previous studies, we have demonstrated that under some operational conditions there is a competition between ZVI mediated reduction and Fenton mediated oxidation in the degradation mechanism of an azo dye [18].

The use of iron nanoparticles for the reduction of several contaminants has been widely studied due to the higher specific area and reactivity compared to conventional micrometric iron [19,20]. In this context, the use of nZVI particles was recently proposed to improve the performance of ZVI-assisted Fenton systems [21–23]. However there is evidence in literature that the size of iron particles could affect oxidant utilization, since smaller particles tend to be less efficient due to the higher H_2O_2 consumption by direct reaction with ZVI [24]. Therefore, despite their higher surface area and reactivity, Fe° nanoparticles (nZVI) could be less efficient for pollutant removal than conventional micrometric iron powder (pZVI) in ZVI-Assisted Fenton systems.

The objective of the present work is to assess the advantages and drawbacks of the utilization of nanoparticles in ZVI-Assisted Fenton treatments. The transformation of 4-phenylazophenol (4-PAP), which is a good model pollutant for following the degradation pathways of azo dyes due to the simplicity on its molecular structure, was studied in the presence nZVI or pZVI under different conditions. In particular, we have focused on the competition between H_2O_2 and 4-PAP for the reducing power of micro- and nano- sized ZVI under different working conditions. To the best of our knowledge, this is the first study involving the elimination of 4-PAP by ZVI-mediated reduction and/or by oxidation in ZVI-assisted Fenton systems.

2. Material and methods

2.1. Reagents

4-Phenylazophenol (Alpha Aesar, 98 %), H_2O_2 (Merck, 30 %), $FeSO_4.7H_2O$ (Cicarelli, analytical degree), $NaBH_4$ (98.5 %, Riedel-de Haën), Electrolytic ZVI powder (Anedra, > 98 %) and 2-Propanol (Emsure, analytical degree) were used as provided. H_2SO_4 and NaOH were provided by Merck. All the solutions were prepared using water of Milli-Q grade (Milipore, 18.2 MOmhs.cm at 25 °C).

2.2. Nanosized ZVI synthesis

nZVI was obtained by borohydride reduction of a ferrous salt, based on the method reported by Lien et al. [25]. Briefly, 200 mL of an aqueous solution of $FeSO_4.7H_2O$ 7.5 % p/p at pH 4.0 was purged with N_2 during 20 min. Maintaining N_2 bubbling, 200 mL of a 2 % p/p of $NaBH_4$ at pH = 10 were added drop by drop at a constant velocity of 3 mL min^{-1}, stirring the solution at 20 °C. The nZVI obtained was magnetically separated and washed 2 times with mili-Q water and 2 times with ethanol, dried under vacuum at 60 °C with a rotavapor and stored in a N_2 atmosphere until use. With these procedures, it is

expected to obtain particles of around 50 ± 15 nm [19].

2.3. Experimental procedure

Batch experiments were conducted in a 250 mL pyrex® reactor. 4-Phenylazophenol solutions were prepared at a concentration of 0.1 mM. The initial pH was adjusted by dropwise addition of 0.1 M H_2SO_4 and/or 0.1 M NaOH. No buffers were used in order to avoid potential interferences with Fenton reaction. H_2O_2 and ZVI (nano- or micro- sized) were sequentially added in order to start reaction. At desired times, samples (1.0 mL) were withdrawn and mixed with 1.0 mL of methanol 25 % to prevent composition changes between sampling and analysis [10]. All the experiments were carried out at room temperature and under vigorous magnetic stirring. Samples were passed through 0.45 μm filters (Whatman) before analysis. After filtration, H_2O_2 was measured using a semiquantitive MQuant peroxidase test.

2.4. Analytical techniques

4-PAP concentration measurements were performed by HPLC with a Thermo Scientific Dionex UltiMate 3000™ instrument equipped with a vacuum degasser, a quaternary pump, an autosampler and UV–vis diode array detector. Separation was performed on a Fortis C18 (250 mm x 2.1 mm, i.d.: 5 μm) column. The injection volume was 20 μL. A mixture of 50 % acetate buffer (0.01 M, pH = 4.8) and 50% acetonitrile was used as elution phase with a flow rate of 1 mL.min^{-1}. 4-PAP retention time is 5.8 min on these conditions and the area of the signal obtained at 347 nm was used for quantification.

Degradation products of 4-PAP were analyzed by both LC-MS and CG-MS. LC-MS runs were performed on a Shimadzu instrument (solvent delivery module LC-20AB, online degasser DGU-20A3, column oven CTO-20A and autosampler SIL-20A, LC-MS-2010 EV mass detector) equipped with an C18 column (150 × 4.6 mm, 5 μm particle size, Restek, USA). The column temperature was maintained at 30.0 ± 0.2 °C. An isocratic mobile phase composed of 50/50 (v/v) ACN/0.1 % formic acid in water was used, with a flow rate of 0.3 mL.min^{-1}. M/Z detector was set at 199, 94, 110, 215, and 231 to identify 4-PAP and its primary degradation products (aniline, 4-OH-aniline, monohydroxylated and dihydroxylated derivatives of 4-PAP). In order to quantify the signal of the latter compounds, integration at the desired M/Z relation was carried out. Samples for CG-MS analysis were extracted with hexane and analyzed in a Trace GC Ultra instrument (Thermo Scientific, Waltham, MA, USA) coupled to an ISQ mass spectrometer controlled by a computer running X-Calibur software. Aliquots of 1 μL were injected using an AI/AS 3000 auto sampler (Thermo Scientific). In splitless mode, the injector temperature was maintained at 250 °C. The separation was carried out using a Thermo Scientific™ TRACE™ TR-5MS column (30 mm × 0.25 mm × 0.25 μm) and helium (purity > 99.9%) as the carrier gas (flow rate of 1 mL min^{-1}). GC oven temperature program was as follows: initial temperature of 60 °C for 1 min, 10 °C min^{-1} to 130 °C, 4 °C min^{-1} to 230 °C, and finally 8 °C min^{-1} to 250 °C (held for 10 min). The ion source and transfer line temperature were kept at 250 and 280 °C, respectively. Electron ionization mass spectra at m/z of 50–500 were recorded at 70 eV.

Specific surface area of pristine ZVI particles was determined by N_2 adsorption at 77 K using a Micromeritics ASAP 2020 instrument.

3. Results

3.1. Kinetic profiles of 4-PAP degradation

In order to compare pZVI and nZVI performance for the degradation of 4-PAP, kinetic profiles were studied with and without H_2O_2 under different initial conditions. Fig. 1 shows the behavior of these systems when operated at an initial pH of 3.00. The comparison between the
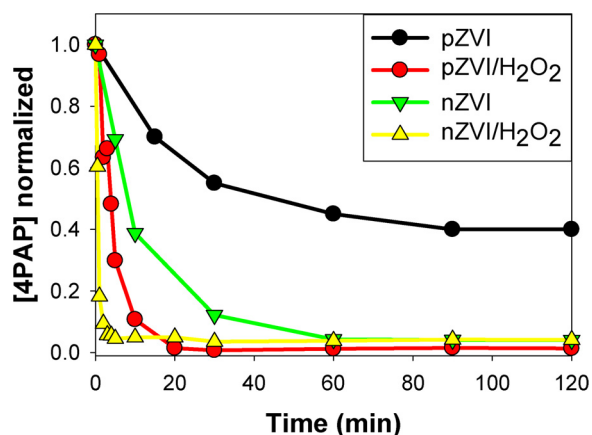
Fig. 1. Kinetic profiles for 4-PAP degradation with ZVI at starting pH of 3.00. Initial conditions: [4-PAP] = 0.1 mM, pH = 3.00, [H_2O_2] = 2.0 mM, ZVI = 0.20 g/L.

results obtained with nZVI and pZVI in the absence of H_2O_2 shows that nZVI completely removed the dye during the first hour of reaction, while pZVI was unable to remove more than 60% of 4-PAP under the tested conditions. Taking into account the results obtained from N_2 adsorption at 77 K, the higher removal rate of nZVI may be ascribed to its high specific surface area (62.28 m^2/g) compared to that of pZVI (0.67 m^2/g). Moreover, if the amount of pZVI is increased to match the area of the nZVI particles in the same conditions, no difference on degradation rates of 4-PAP between both ZVI sources is observed (Fig. S2). Therefore, under the latter conditions, nZVI is a more efficient material than the micrometric powder because of its higher exposed area, the specific reactivities of both materials being rather similar.

Upon external addition of H_2O_2 to the reaction mixture, an enhancement of 4-PAP degradation occurs due to the contribution of the Fenton oxidation pathway. In this case, nZVI also showed a better performance than pZVI, which can be attributed mainly to the faster generation of Fe(II) during Fe° corrosion as consequence of its higher exposed surface. It is important to highlight that, when systems were operated at the starting pH of 3.00, both pZVI/H_2O_2 and nZVI/ H_2O_2 systems were more efficient for 4-PAP degradation than a traditional Fenton system where iron was added on the form of a ferrous salt (Fig. S3A). Given the rather short timescales required for complete 4-PAP elimination in the presence of H_2O_2, the improvement observed by the use of ZVI sources instead of Fe(II) cannot be explained by the contribution of ZVI mediated reduction. A possible explanation is that the constant release of Fe(II) from ZVI prevents the presence of high concentrations of Fe(II) in solution, which may result in the scavenging of HO· radicals [26].

It is well known that ZVI performance is strongly dependent on pH conditions [27–30]. Therefore, it is interesting to compare the behavior of both ZVI sources when system is operated in mild acidic conditions (i.e. at starting pH of 5.00, Fig. 2). Comparison between kinetic profiles obtained in ZVI assisted systems with initial pH values of 3.00 and 5.00 (Figs. 1 and 2) shows that 4-PAP elimination rates decrease as the initial pH is raised. The decrease of the rates of both reduction and oxidation as the working pH is increased maybe ascribed to the precipitation of Fe (III) in the form of oxyhydroxides onto ZVI surfaces [18]. This precipitation produces a corrosion layer, which prevents substrate reduction onto ZVI surface and also reduces the release of Fe(II) species to the solution bulk that are necessary for homogeneous Fenton reaction [31]. In order to evaluate the role of the corrosion layer on nZVI and pZVI materials, additional experiments were conducted in the presence of EDTA, which forms highly stable complexes with Fe(III) (K_{cond} = $3.2.10^{13}$ M^{-1}) [32] thus preventing Fe(III) oxyhydroxides precipitation [18]. The enhancement of 4-PAP elimination in the presence of EDTA (Fig. 2), suggests that the formation of the corrosion layer plays a

significant role on the decrease of substrate transformation rates induced by both materials.

It is interesting to notice that, at pH 5.00 and in the absence of EDTA, the higher 4-PAP elimination rate was recorded for nZVI without H_2O_2 addition, while no significant transformation was observed for the nZVI/H_2O_2 system (Fig. 2). This behavior contrasts with that observed when the initial pH was 3.00 (Fig. 1). It is worth mentioning that, although 4-PAP is not transformed at an initial pH of 5.00, hydrogen peroxide decays quickly, [H_2O_2] being below the detection limit after the first 2 min. The latter result may be explained by taking into account the reaction of H_2O_2 with nZVI surface (Reaction 3).

$$Fe^0 + H_2O_2 + 2 H^+ \rightarrow Fe(II) + 2 H_2O \quad (\Delta E° = 2.223 \, V) \qquad (3)$$
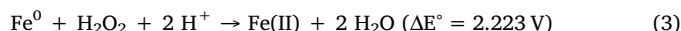
Therefore, the addition of H_2O_2 in the presence of nZVI suspensions at mild acidic conditions exerts a negative effect on the efficiency of 4-PAP elimination because reaction 3 causes a decrease in Fe° sites available to reduce 4-PAP. This effect will be discussed further in Section 3.3. In addition, it was previously reported that in mild acidic conditions, reaction 3 becomes the main route of H_2O_2 consumption for ZVI-assisted systems [18], which reduces oxidant availability for Fenton reaction.

In the case of pZVI, an almost negligible degradation was observed in the absence of H_2O_2, while 4-PAP elimination was significant upon addition of H_2O_2 (Fig. 2). In these conditions, oxidant consumption is slower and H_2O_2 is still present after 120 min of reaction, although in a low concentration (< 0.5 ppm). The effect of H_2O_2 addition for pZVI source at this pH condition is opposite to the one observed for nZVI. The differences may be explained by considering that the higher surface area of nZVI makes them more suitable for promoting the reduction of the substrate, but also more susceptible to directly react with H_2O_2, thus consuming the oxidant and promoting iron passivation. From a technological viewpoint, worthless consumption of H_2O_2 through reaction 3 represents a very important issue for ZVI assisted Fenton systems since it leads to a much less efficient use of the oxidant in comparison with the traditional Fe(II)/H_2O_2 Fenton systems (Fig. S3B). Although this is true for both ZVI sources, this effect is especially noticeable for the case of nZVI.

The higher nZVI corrosion upon addition of H_2O_2 is also evidenced by the recorded pH profiles (Fig. S4), since pH sharply increases from 5.0 to more than 8.0 within the first 5 min of reaction. At this pH, Fe(II) is highly unstable and tends to oxidize to Fe(III) species, which precipitate and become unable to sustain Fenton-like processes. On the other hand, for the pZVI/H_2O_2 system the solution pH increases slowly and does not exceed a value of 6.4, thus allowing the oxidation of 4-PAP to some extent.

3.2. Product analysis

The formation of 4-PAP byproducts by nZVI and pZVI were analyzed by LC-MS and CG-MS. The results obtained in the absence of externally added H_2O_2 are shown in Fig. 3. For the experiments conducted with an initial pH of 3.00, fragments compatible with the ionized form of aniline and 4-OH-aniline were identified by LC-MS and confirmed by CG-MS as the unique detectable products for both ZVI sources. In contrast, for the experiments conducted with an initial pH of 5.00, the profiles of 4-PAP byproducts were much more dependent on the ZVI source used. In the presence of nZVI 4,4′-dihydroxyazobenzene (MOH-4-PAP) was detected along with aniline and 4-OH-aniline; while in the presence of pZVI only MOH-4-PAP was detected as 4-PAP byproduct with the extent of 4-PAP degradation being rather low (i.e. less than 5% of 4-PAP degradation after 2 h of reaction, Fig. 2). The formation of MOH-4-PAP under mild acidic conditions could be accounted for by the fact that the reduction of dissolved oxygen by passive iron surfaces produces H_2O_2 "in situ" [33–35], thus leading to the generation of oxidizing species through the Fenton reaction.
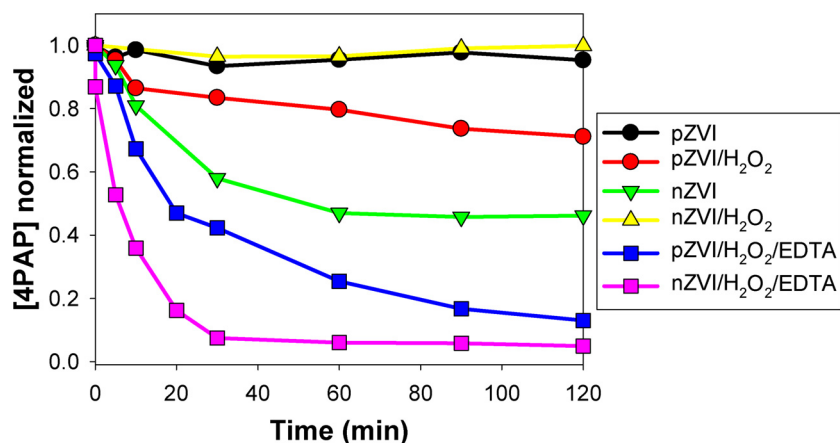
Fig. 2. Kinetic profiles for 4-PAP degradation with ZVI at starting pH of 5.00. Initial conditions: [4-PAP] = 0.1 mM, pH = 5.00, [H_2O_2] = 2.0 mM, ZVI = 0.20 g/L, [EDTA] = 36 mM.

In the presence of added H_2O_2 a wide variety of oxidation by-products derived from hydroxylation reactions were found. Mono- and di-hydroxylated derivatives of 4-PAP formed by OH$^{\bullet}$ addition to the aromatic ring (MOH-4-PAP and DOH-4-PAP, respectively) were detected by LC-MS. CG-MS analyses confirmed that MOH-4-PAP match to a product were HO$^{\bullet}$ attack is produced on the non-hydroxylated ring of 4-PAP, mainly on para- position to form the 4,4′-dihydroxyazobenzene. Aniline and 4-OH-aniline were also detected on systems operated at starting pH of 3.00, thus confirming that ZVI mediated reduction is also present when H_2O_2 is added, although its contribution is negligible.

The inspection of the distribution of reaction products for pZVI/ H_2O_2 systems (Fig. 4) evidenced that 4-PAP hydroxylated derivatives are the main reaction intermediaries. The latter results show that, under both pH conditions, oxidation is the main 4-PAP transformation pathway when pZVI is used as iron source. Owing to the difference in the overall reaction rates, when working at starting pH of 3.00 MOH-4-PAP and DOH-4-PAP are completely degraded after 60 min of reaction, while at pH 5.00 they are still present in the reaction mixture for more than 120 min. In case of nZVI/H_2O_2 system, depending on initial pH a different behavior is observed. For the experiment performed with an initial pH of 3.00, the main products detected are MOH-4-PAP and DOH-4-PAP (Fig. 4), indicating that oxidation triggered by Fenton reaction is the main degradation pathway. However, for the system operated with an initial pH of 5.00 the main products correspond to the amines formed by the reduction of 4-PAP, and only traces of the hydroxylated derivatives appear after 30 min (Fig. 4). The latter results suggest that, under these conditions, the rather small reaction progress observed (Fig. 2) is mostly associated to the ZVI mediated reduction of 4-PAP, since the addition of H_2O_2 does not lead to any significant oxidation of the substrate.
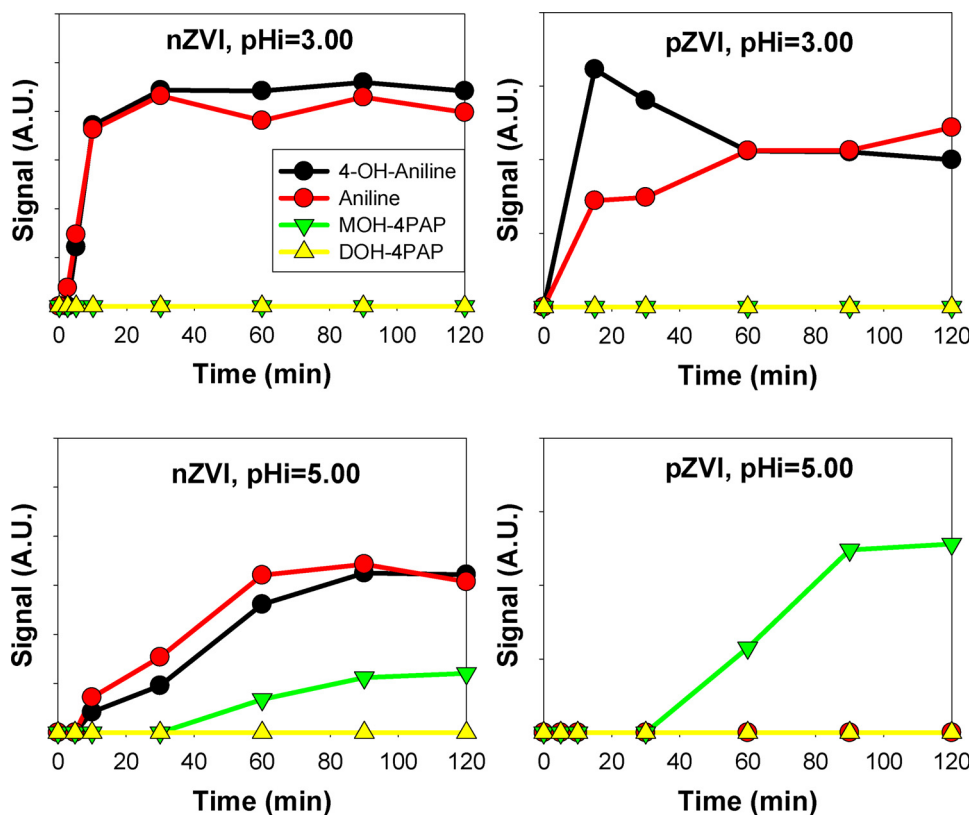

Fig. 3. Profiles of 4-PAP byproducts obtained by LC-MS in the absence of H_2O_2. Initial conditions: [4-PAP] = 0.1 mM, ZVI = 0.20 g L^{-1}.
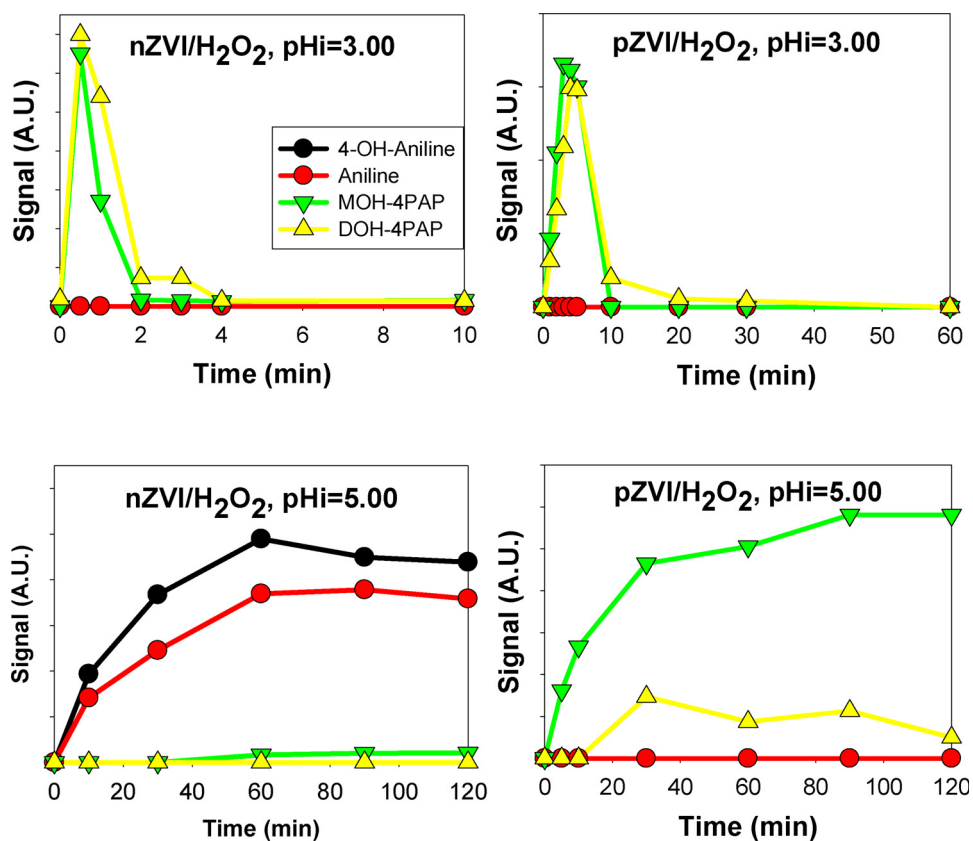
Fig. 4. Profiles of 4-PAP byproducts obtained by LC-MS with H_2O_2 addition. Initial conditions: [4-PAP] $= 0.1$ mM, ZVI $= 0.20$ g L^{-1}, [H_2O_2] $= 2.0$ mM.
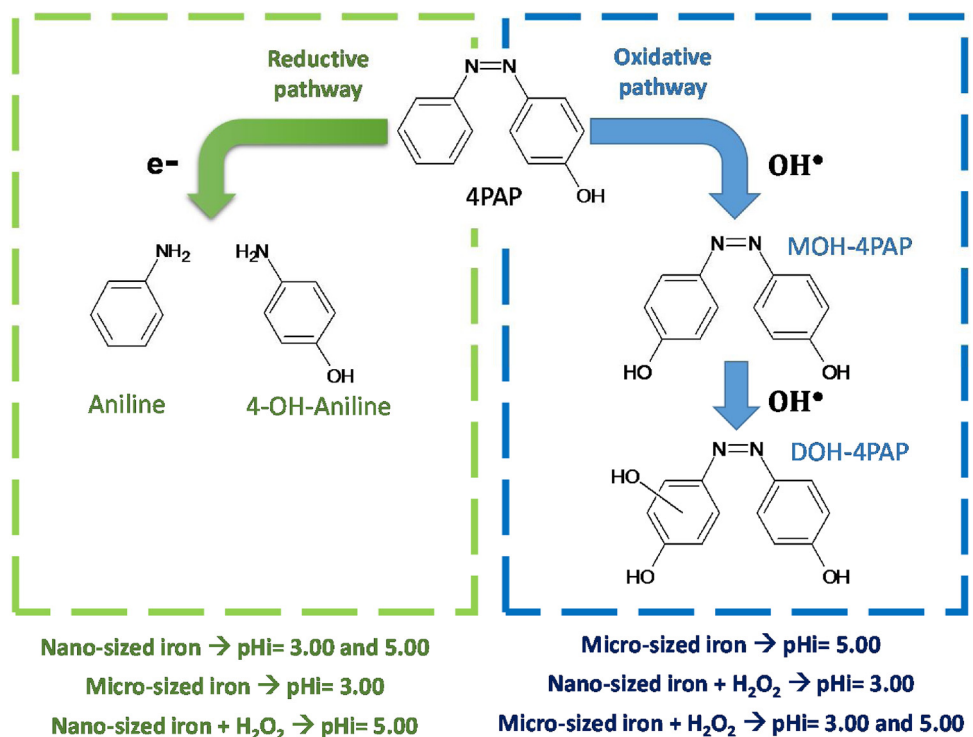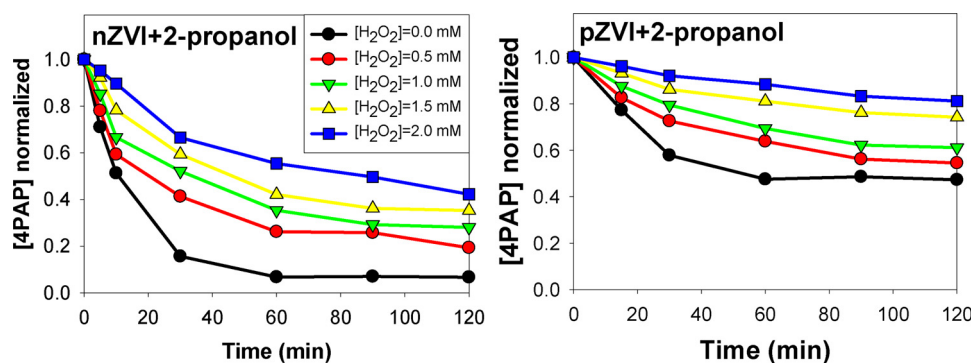

Fig. 5. Scheme of main degradation products followed by LC-MS.

Fig. 6. Isopropanol inhibition of Fenton oxidation for nZVI (left) and pZVI (right). Initial conditions: [4-PAP] = 0.1 mM, pHi = 3.00, [H_2O_2] = 0–2.0 mM, ZVI = 0.20 g/L, [2-propanol] = 0.5 M.

Main degradation products detected for each system studied, as well as their formation pathways, are schematized on Fig. 5.

3.3. 4-PAP degradation in the presence of 2-propanol

The role of OH· radicals was evaluated by adding 2-propanol as scavenger since it has been reported that it can react with both homogenous and surface bonded OH· [22]. If the oxidation of 4-PAP in ZVI assisted systems is triggered by OH· radicals, then the presence of 2-propanol should inhibit Fenton oxidation pathway. It is important to mention that, we have recently shown that ferryl ions have a negligible contribution on the oxidation of Acid Black 1 under the conditions used in the present work [32]. Fig. 6 compares the kinetics of 4-PAP elimination obtained using nZVI and pZVI in the presence of 2-propanol and using different concentrations of H_2O_2. The decay profiles recorded in the absence of H_2O_2 are similar to those obtained in the absence of 2-propanol (Fig. 1) confirming that the presence of the scavenger does not hinder the reduction pathway. In addition, for the all tested H_2O_2 concentrations, only aniline and p-OH-aniline, which come from reductive pathways, were found by LC-MS as degradation byproducts. The absence of oxidation products in the presence of 2-propanol supports the hypothesis that HO· radicals are the main reactive species involved in 4-PAP oxidation at pH 3.00. Interestingly, kinetic profiles of Fig. 6 show a progressive decrease in both the rate and the degree of 4-PAP transformation as [H_2O_2] is increased. This behavior can be explained by considering that H_2O_2 is an electron acceptor than can compete with 4-PAP for the electrons released by ZVI. Moreover, the results obtained in the presence of 2-propanol suggest that the increase of H_2O_2 concentration in acidic media not only may enhance the rate of 4-PAP oxidation triggered by Reaction 1 but also may decrease, to some extent, the iron-mediated reduction of 4-PAP (Reaction 2) due to the increased ZVI consumption through Reaction 3.

4. Conclusions

The use of two different sources of metallic iron pZVI and nZVI for the elimination of 4-PAP under different conditions allowed us to address several mechanistic and kinetic issues regarding the application of ZVI based technologies. Although both nanometric and micrometric particles showed similar transformation products (derived from azo bond reduction or HO· mediated oxidation), the relative contributions of reductive and oxidative pathways as well as the overall elimination rates significantly depend on the ZVI source, especially under mild acidic conditions (i.e. pHi 5.00).

In the absence of added H_2O_2 and for moderate acidic media (i.e. pHi 3.00), nZVI exhibited a faster substrate removal than pZVI, the main mechanism involved in 4-PAP transformation for both ZVI sources being the azo bond reduction with the formation of the corresponding amines. Results show that the higher efficiency recorded for the

nanoscaled material may be fully ascribed to its higher exposed area, since the specific reactivities of both materials are very similar. In contrast, for mild acidic media (i.e. pHi = 5.00) the formation of a corrosion layer onto iron particles may substantially reduce surface reactivity. The latter effect is much less critical for nZVI than for pZVI since the higher surface area of nanoparticles makes the substrate reduction possible even in mild acidic media. This behavior is one of the main advantages of the use of nanoparticulated ZVI for reductive elimination. It should be taken into account that, for ZVI systems operated under mild pH conditions, the "in situ" formation of H_2O_2 leads to the contribution of oxidative transformation pathways. Moreover, in these conditions, the transformation of 4-PAP by nZVI occurred through both reductive and oxidative pathways transformation, whereas for the pZVI only oxidation products of 4-PAP where found.

The presence of added H_2O_2 leads, for moderate acidic media, to faster transformation rates due to hydroxyl radicals mediated oxidation of 4-PAP, the major transformation products detected being the mono- and di-hydroxylated derivatives of the target substrate, independently of the source of ZVI used. It is important to highlight that, under moderate acidic conditions, both pZVI/H_2O_2 and nZVI/H_2O_2 systems were more efficient for 4-PAP elimination than a traditional Fenton system. As the working pH is raised, a strong dependence of the dominant transformation pathway on the ZVI source used is evidenced. For pZVI, the addition of H_2O_2 under mild acidic conditions produced a complete inhibition of the reduction pathway, being the oxidation the main degradation mechanism. In contrast, for the same working pH, nZVI/H_2O_2 systems showed an almost negligible substrate transformation mainly driven by 4-PAP reduction.

The results obtained in the present work suggest that the higher reactivity of ZVI nanoparticles compared to conventional powder may be, under some pH conditions, a drawback for ZVI-assisted oxidation treatments. The better understanding of the advantages and disadvantages of each iron source allows a more rational design of ZVI-based treatments. Noteworthy, despite this work has been focused on the degradation of a model azo dye, many of the insights obtained could also be applicable to other types of organic substrates. In particular, the competition between reduction and oxidation pathways is also expected to occur with other reducible compounds such as chlorinated solvents or nitroaromatic contaminants.

Funding sources

CRediT authorship contribution statement

Jorge A. Donadelli: Conceptualization, Methodology, Formal analysis, Investigation, Writing - original draft, Writing - review & editing, Visualization. **Bruno Caram:** Investigation. **Maria Kalaboka:** Investigation. **Margarita Kapsi:** Investigation. **Vasilios A. Sakkas:** Resources, Writing - review & editing, Project administration, Funding acquisition. **Luciano Carlos:** Resources, Writing - review & editing, Supervision, Project administration, Funding acquisition. **Fernando S. García Einschlag:** Resources, Writing - review & editing, Supervision, Funding acquisition.

Declaration of Competing Interest

The authors declare no competing financial interest.

Acknowledgment

Appendix A. Supplementary data

Supplementary material related to this article can be found, in the online version, at doi:https://doi.org/10.1016/j.jece.2019.103624.

References

[1] C. Fernández, M.S. Larrechi, M.P. Callao, An analytical overview of processes for removing organic dyes from wastewater effluents, Trends Anal. Chem. 29 (2010) 1202–1211, https://doi.org/10.1016/j.trac.2010.07.011.

[2] L. Gomathi Devi, S. Girish Kumar, K. Mohan Reddy, C. Munikrishnappa, L.G. Devi, S.G. Kumar, K.M. Reddy, C. Munikrishnappa, Photo degradation of Methyl Orange an azo dye by Advanced Fenton Process using zero valent metallic iron: influence of various reaction parameters and its degradation mechanism, J. Hazard. Mater. 164 (2009) 459–467, https://doi.org/10.1016/j.jhazmat.2008.08.017.

[3] S.-H. Chang, S.-H. Chuang, H.-C. Li, H.-H. Liang, L.-C. Huang, Comparative study on the degradation of I.C. Remazol Brilliant Blue R and I.C. Acid Black 1 by Fenton oxidation and Fe0/air process and toxicity evaluation, J. Hazard. Mater. 166 (2009) 1279–1288, https://doi.org/10.1016/j.jhazmat.2008.12.042.

[4] P.V. Nidheesh, R. Gandhimathi, S.T. Ramesh, Degradation of dyes from aqueous solution by Fenton processes: a review, Environ. Sci. Pollut. Res. 20 (2013) 2099–2132, https://doi.org/10.1007/s11356-012-1385-z.

[5] C. Zaharia, D. Suteu, Textile organic dyes -characteristics, polluting effects and separation/elimination procedures from industrial effluents - A critical overview, Org. Pollut. Ten Years After Stock. Conv. Anal. Updat. (2012) 55–81.

[6] H.M. Pinheiro, E. Touraud, O. Thomas, Aromatic amines from azo dye reduction: Status review with emphasis on direct UV spectrophotometric detection in textile industry wastewaters, Dyes Pigm. 61 (2004) 121–139, https://doi.org/10.1016/j.dyepig.2003.10.009.

[7] S. Collier, J.E. Storm, R.L. Bronaugh, Reduction of azo dyes during in vitro percutaneous absorption, Toxicol. Appl. Pharmacol. 118 (1993) 73–79, https://doi.org/10.1006/taap.1993.1011.

[8] D.A. Nichela, J.A. Donadelli, B.F. Caram, M.M. Haddou, F.J. Rodriguez, E. Oliveros, F.S. García, F.J. Rodriguez Nieto, E. Oliveros, F.S. Garcia, Einschlag, Iron cycling during the autocatalytic decomposition of benzoic acid derivatives by Fenton-like and photo-Fenton techniques, Appl. Catal. B, Environ. 170–171 (2015) 312–321, https://doi.org/10.1016/j.apcatb.2015.01.028.

[9] P. Wardman, Reduction potentials of one-electron couples involving free radicals in aqueous solution, J. Phys. Chem. 18 (1989) 1637–1755, https://doi.org/10.1063/1.555843.

[10] L. Carlos, D. Fabbri, A.L. Capparelli, A.B. Prevot, E. Pramauro, F.S.G. Einschlag, Intermediate distributions and primary yields of phenolic products in nitrobenzene degradation by Fenton's reagent, Chemosphere. 72 (2008) 952–958, https://doi.org/10.1016/j.chemosphere.2008.03.042.

[11] L. Wojnárovits, E. Takács, Irradiation treatment of azo dye containing wastewater: an overview, Radiat. Phys. Chem. 77 (2008) 225–244, https://doi.org/10.1016/j.radphyschem.2007.05.003.

[12] M.A. Meetani, S.M. Hisaindee, F. Abdullah, S.S. Ashraf, M.A. Rauf, Liquid chromatography tandem mass spectrometry analysis of photodegradation of a diazo compound : a mechanistic study, Chemosphere. 80 (2010) 422–427, https://doi.org/10.1016/j.chemosphere.2010.04.065.

[13] B.G. Petri, R.J. Watts, A.L. Teel, S.G. Huling, R.A. Brown, et al., Fundamentals of ISCO using hydrogen peroxide, in: R.L. Siegrist (Ed.), Situ Chem. Oxid. Groundw. Remediat. Springer, New York, 2011, , https://doi.org/10.1007/978-1-4419-7826-4 p. 678.

[14] B. Girit, D. Dursun, T. Olmez-Hanci, I. Arslan-Alaton, Treatment of aqueous bisphenol A using nano-sized zero-valent iron in the presence of hydrogen peroxide and persulfate oxidants, Water Sci. Technol. 71 (2015) 1859–1868, https://doi.org/10.2166/wst.2015.175.

[15] R. Li, X. Jin, M. Megharaj, R. Naidu, Z. Chen, Heterogeneous Fenton oxidation of 2,4-dichlorophenol using iron-based nanoparticles and persulfate system, Chem. Eng. J. 264 (2015) 587–594, https://doi.org/10.1016/j.cej.2014.11.128.

[16] S. Nam, P.G. Tratnyek, Reduction of azo dyes with zero-valent iron, Water Res. 34 (2000) 1837–1845, https://doi.org/10.1016/S0043-1354(99)00331-0.

[17] L. Santos-juanes, F.S.G. Einschlag, A.M. Amat, A. Arques, Combining ZVI reduction with photo-Fenton process for the removal of persistent pollutants, Chem. Eng. J. 310 (2016) 484–490, https://doi.org/10.1016/j.cej.2016.04.114.

[18] J.A. Donadelli, L. Carlos, A. Arques, F.S. García Einschlag, Kinetic and mechanistic analysis of azo dyes decolorization by ZVI-assisted Fenton systems : pH-dependent shift in the contributions of reductive and oxidative transformation pathways, Appl. Catal. B Environ. 231 (2018) 51–61, https://doi.org/10.1016/j.apcatb.2018.02.057.

[19] P. Bardos, B. Bone, D. Elliott, N. Hartog, J. Henstock, A Risk / Benefit Approach to the Application of Iron Nanoparticles for the Remediation of Contaminated Sites in the Environment, (2011).

[20] J. Wu, B. Wang, L. Blaney, G. Peng, P. Chen, Y. Cui, S. Deng, Y. Wang, J. Huang, G. Yu, Degradation of sulfamethazine by persulfate activated with organo- montmorillonite supported nano-zero valent iron, Chem. Eng. J. 361 (2019) 99–108, https://doi.org/10.1016/j.cej.2018.12.024.

[21] T. Shahwan, S. Abu Sirriah, M. Nairat, E. Boyaci, A.E. Eroğlu, T.B. Scott, K.R. Hallam, Green synthesis of iron nanoparticles and their application as a Fenton-like catalyst for the degradation of aqueous cationic and anionic dyes, Chem. Eng. J. 172 (2011) 258–266, https://doi.org/10.1016/j.cej.2011.05.103.

[22] L. Xu, J. Wang, Degradation of 4-Chloro-3,5-Dimethylphenol by a heterogeneous fenton-like reaction using nanoscale zero-valent Iron catalysts, Environ. Eng. Sci. 30 (2013) 294–301, https://doi.org/10.1089/ees.2012.0025.

[23] J. Yan, L. Qian, W. Gao, Y. Chen, D. Ouyang, M. Chen, Enhanced Fenton-like Degradation of Trichloroethylene by Hydrogen Peroxide Activated with Nanoscale Zero Valent Iron Loaded on Biochar, Sci. Rep. 7 (2017) 1–9, https://doi.org/10.1038/srep43051.

[24] S. Rodriguez, L. Vasquez, A. Romero, A. Santos, Dye oxidation in aqueous phase by using zero-valent Iron as persulfate activator: kinetic model and effect of particle size, Ind. Eng. Chem. Res. 53 (2014) 12288–12294, https://doi.org/10.1021/ie501632e.

[25] H.-L. Lien, D.W. Elliott, Y.-P. Sun, W.-X. Zhang, Recent progress in zero-valent Iron nanoparticles for groundwater remediation, J. Environ. Eng. Manag. 16 (2006) 371–380.

[26] C. Lin, Y. Chen, Feasibility of using nanoscale zero-valent iron and persulfate to degrade sulfamethazine in aqueous solutions, Sep. Purif. Technol. 194 (2018) 388–395, https://doi.org/10.1016/j.seppur.2017.10.073.

[27] C. He, J. Yang, L. Zhu, Q. Zhang, W. Liao, S. Liu, Y. Liao, M.A. Asi, D. Shu, pH-dependent degradation of acid orange II by zero-valent iron in presence of oxygen, Sep. Purif. Technol. 117 (2013) 59–68, https://doi.org/10.1016/j.seppur.2013.04.028.

[28] C.H. Weng, Y.T. Lin, C.K. Chang, N. Liu, Decolourization of direct blue 15 by Fenton/ultrasonic process using a zero-valent iron aggregate catalyst, Ultrason. Sonochem. 20 (2013) 970–977, https://doi.org/10.1016/j.ultsonch.2012.09.014.

[29] J. Fan, Y. Guo, J. Wang, M. Fan, Rapid decolorization of azo dye methyl orange in aqueous solution by nanoscale zerovalent iron particles, J. Hazard. Mater. 166 (2009) 904–910, https://doi.org/10.1016/j.jhazmat.2008.11.091.

[30] Y. He, J.F. Gao, F.Q. Feng, C. Liu, Y.Z. Peng, S.Y. Wang, The comparative study on the rapid decolorization of azo, anthraquinone and triphenylmethane dyes by zero-valent iron, Chem. Eng. J. 179 (2012) 8–18, https://doi.org/10.1016/j.cej.2011.05.107.

[31] Y.H. Huang, T.C. Zhang, Effects of dissolved oxygen on formation of corrosion products and concomitant oxygen and nitrate reduction in zero-valent iron systems with or without aqueous Fe2+, Water Res. 39 (2005) 1751–1760, https://doi.org/10.1016/j.watres.2005.03.002.

[32] J.A. Donadelli, L. Carlos, A. Arques, F.S. García Einschlag, Kinetic and mechanistic analysis of azo dyes decolorization by ZVI-assisted Fenton systems: pH-dependent shift in the contributions of reductive and oxidative transformation pathways, Appl. Catal. B Environ. 231 (2018) 51–61, https://doi.org/10.1016/j.apcatb.2018.02.057.

[33] V. Jovancicevic, J.O.M. Bockris, The mechanism of oxygen reduction on Iron in neutral solutions, J. Electrochem. Soc. 133 (1986) 1797–1807, https://doi.org/10.1149/1.2109021.

[34] T. Harada, T. Yatagai, Y. Kawase, Hydroxyl radical generation linked with iron dissolution and dissolved oxygen consumption in zero-valent iron wastewater treatment process, Chem. Eng. J. 303 (2016) 611–620, https://doi.org/10.1016/j.cej.2016.06.047.

[35] S. Jagadevan, M. Jayamurthy, P. Dobson, I.P. Thompson, A novel hybrid nano zerovalent iron initiated oxidation - Biological degradation approach for remediation of recalcitrant waste metalworking fluids, Water Res. 46 (2012) 2395–2404, https://doi.org/10.1016/j.watres.2012.02.006.